

(1971).

<sup>4</sup>Hubert M. James, Phys. Rev. **164**, 1153 (1967).<sup>5</sup>D. E. Polk, J. Non-Cryst. Solids **5**, 365 (1971).<sup>6</sup>C. L. Mallows, J. Roy. Stat. Soc. **B18**, 139 (1956).<sup>7</sup>C. L. Mallows, Proc. London Math. Soc. **13**, 385 (1963).<sup>8</sup>T. M. Donovan and W. E. Spicer, Phys. Rev. Letters **21**, 1572 (1968).<sup>9</sup>D. T. Pierce and W. E. Spicer, Phys. Rev. Letters **27**, 1220 (1971).<sup>10</sup>T. E. Fisher and M. Erbudak, Phys. Rev. Letters **27**, 1220 (1971).<sup>11</sup>M. F. Thorpe and D. Weaire, Phys. Rev. Letters **27**, 1581 (1971).<sup>12</sup>See, e.g., R. Bellman, *Introduction to Matrix Analysis* (McGraw-Hill, New York, 1960), p. 278.

PHYSICAL REVIEW B

VOLUME 6, NUMBER 6

15 SEPTEMBER 1972

## Flatband Electroreflectance of Gallium Arsenide. I. Experimental Results\*

Stephen F. Pond<sup>†</sup> and Paul Handler

*Department of Physics and Materials Research Laboratory,  
University of Illinois, Urbana, Illinois 61801*

(Received 20 December 1971)

The electroreflectance (ER) spectrum of *n*-type gallium arsenide in the 1.2–5.3-eV photon energy range has been measured. It was found from examination of the direct-edge  $\Delta\epsilon_1$  line shapes and collaborative differential capacitance measurements that quite uniform fields were obtained. The interference between the light- and heavy-hole contributions to the ER signal at  $E_0$  was observed. The data were obtained using the electrolyte technique with potentiostatic control. The condition of no space-charge region, flatband, was determined by utilizing the even field dependence of the Franz-Keldysh effect. Square-wave modulation of the space charge from the flatband condition to several depletion-field values was used for the data presented. The ER line shapes at the direct edge provided a means for determining the importance of field inhomogeneity and broadening effects as well as a determination of electric field values.  $\Delta\tilde{\epsilon}$  was computed from a Kramers-Kronig transformation of  $\Delta R/R$ .

### I. INTRODUCTION

Electroreflectance<sup>1,2</sup> is a powerful technique for studying the properties of electrons in semiconductors. However, reliable, quantitative information can be obtained from electroreflectance (ER) data only if the influence of several experimental factors is understood. The most important shortcoming of the past ER studies on GaAs<sup>3–14</sup> was the failure to reliably characterize the position of the energy bands during the modulation cycle. Quantitative analysis can be performed on ER data only if the flatband position is known relative to the band-bending produced by the electric field modulation. Also, in many of the earliest experiments,<sup>3–10</sup> sine-wave modulations were used which, due to the nonlinearity inherent in the electro-optic response, further complicate any attempt to quantitatively analyze the resulting line shapes. In most of the past surface-barrier ER studies<sup>3,4,8–11,14</sup> large peaks at photon energies just below the expected direct-gap energy  $E_0$  were observed. This structure, variously attributed to impurity states, surface states, or backface reflections, is not well understood. In addition, field inhomogeneity and broadening can be seen to be important factors in many of these past experiments<sup>3,5,8–11,14</sup>; the line shapes reported are distorted and exhibit only a few half-oscillations. Transverse ER work on

GaAs<sup>6,12,13</sup> should not exhibit effects due to spatial field variation. However, these line shapes<sup>6,12,13</sup> do appear just as distorted as the surface-barrier line shapes. As a result of the shortcomings mentioned above, efforts to fit a theoretical line shape to the experimental data have been reported in only three cases,<sup>2,11,12</sup> the results of which have been largely unsuccessful.

We report here ER data for GaAs which is as well characterized and useful for quantitative analysis as that previously obtained for Ge.<sup>15–17</sup> The apparatus and procedures, particularly the method for measuring flatband and certain electrochemical considerations, are discussed in Sec. II. In Sec. III we present data taken over a 1.2–5.3-eV photon energy range. The direct-edge data are used to calibrate the experiment, i.e., to determine the importance of factors such as field inhomogeneity, broadening, and dc bias potential. In Sec. IV we summarize the important claims and conclusions. A quantitative analysis of the data will be presented in a subsequent paper.<sup>18</sup>

### II. EXPERIMENTAL

A block diagram of the apparatus is shown in Fig. 1. The system is similar to others previously described in the literature.<sup>19,20</sup> Two new features, a provision for cooling the electrolyte and a method of monitoring the flatband (zero-field) bias condi-

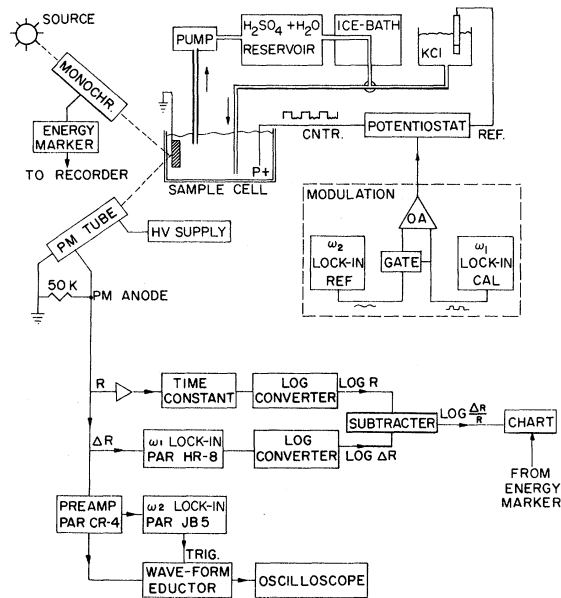


FIG. 1. Block diagram of the experimental setup.

tion, have been added. As a practical matter, ER data can best be understood quantitatively if the modulating voltage is a square wave with one-half cycle at the flatband voltage and the other half-cycle at either a depletion- or accumulation-field voltage.

#### A. Flatband Determination

The modulation system shown in Fig. 1 was designed to enable the determination of the flatband voltage bias by utilizing the even-field-dependence property of the Franz-Keldysh effect.<sup>21</sup> A sine-wave modulation of frequency  $\omega_2$  was superposed on one-half of a square-wave modulation of  $\omega_1$ . Typically the amplitude of the sine wave was 50 mV peak to peak and  $\omega_2 \approx 2.5\omega_1$ . The dc level of the voltage applied to the sample was then adjusted until the sine-wave modulation just straddled the flatband voltage. When this happens, the even-field Franz-Keldysh effect will show no response at the modulation frequency  $\omega_2$  but will exhibit a signal at  $2\omega_2$  (and higher even harmonics of  $\omega_2$ ). The vanishing of the ER response at the sine-wave fundamental  $\omega_2$  was observed with a lock-in amplifier. A Princeton Applied Research waveform eductor was also used to examine the  $\omega_2$  component of the ER signal. The eductor was used to ensure that zeros seen on the  $\omega_2$  lock-in amplifier were accompanied by strong  $\sin(2\omega_2)$  waveforms. We have observed situations where changing the dc bias of the sample moved the zeros of the detected  $\Delta R$  signal in such a way that the  $\omega_2$  lock-in indicated a zero signal. The eductor signal in this case does not show a strong  $\sin(2\omega_2)$  waveform.

Furthermore, the ER line shapes at the direct edge show much distortion from the expected shape (an electro-optic  $G_3$  function<sup>22,23</sup>) for these false flatband zeros.

The accuracy of the flatband determination is limited by a few important factors. First, the method assumes that the ER response to the sine-wave modulation is perfectly even in the applied modulation. Thus, a given voltage magnitude must produce a field of equal magnitude and spatial profile on both the accumulation and depletion sides of flatband. This situation will be approximated only for very small modulations, on the order of a few tens of millivolts for GaAs. Also, linear-field electro-optic effects<sup>13</sup> must be small in relation to the Franz-Keldysh effect. Aspnes and Frova<sup>20</sup> have examined the accuracy of the ER-flatband-determination method for the nearly intrinsic Ge:K<sub>2</sub>SO<sub>4</sub> electrolyte system. They found a  $17 \pm 7$  mV difference between the ER flatband determination and a determination combining photovoltage and capacitance measurements. Even smaller differences were found for their more highly doped samples. Independent measurements of the flatband conditions for our *n*-type-GaAs sulfuric-acid-electrolyte system have been made by capacitance measurements. These measurements agree with the ER determination; however, because the GaAs used is strongly extrinsic, the capacitance technique gives at best  $\pm 40$ -mV accuracy. The combination capacitance-photovoltage determination used by Aspnes and Frova<sup>20</sup> will not give better results for our system because of the large excess carrier concentrations and the large surface-recombination velocities of  $10^{16}$ -cm<sup>-3</sup> *n*-type GaAs.<sup>24</sup> Thus, we believe that the ER determination of flatband is as good as any method available. With the sine-wave modulations used, about 50 mV, peak to peak, there could be an error of  $\pm 25$  mV in the flatband voltage bias. This error is unimportant because the small sine wave is being used merely to position a square wave of a few volts. The ER response at the square-wave frequency is dominated by the high-field half of the modulation cycle<sup>20</sup> and is unaffected by small changes of the dc voltage bias. Of course, for small square-wave modulations the ER response is noticeably affected by small changes in the dc bias.

Because small modulations must be used for the sine wave to minimize errors, the response at twice the modulation frequency will be small. It has been our experience that the  $2\omega_2$  signal is large enough to be seen above the noise only at the photon energy of maximum  $\Delta R$  signal for a given critical point. In spite of the above limitations we have been able to monitor flatband at all of the critical-point structure observed.

### B. Electrochemical Considerations

Choosing the proper electrolyte to use with a particular semiconductor is one of the most crucial factors in electrolyte ER. Sulfuric acid in water was found to be an ideal electrolyte for use with *n*-type GaAs. For this system the following situation exists. For zero applied voltage, the GaAs conduction and valence bands are bent up into depletion at the surface. This equilibrium band bending in III-V semiconductors is thought to be due to a large number of surface states which fix the Fermi level at the surface about  $\frac{1}{3}$  of the gap energy away from the top of the valence-band maximum.<sup>25</sup> Flatband is reached by applying a negative voltage bias of approximately 1 V (measured with respect to a calomel electrode in saturated KCl and is accompanied by cathodic current. Positive voltage bias bends the bands further into depletion and is accompanied by anodic current. The conventional explanation for the electrochemical behavior of this system is as follows.<sup>26</sup> When the bands are in depletion and anodic current is observed, minority carriers (holes) are driven towards the interface. In the dark their concentration is very low since  $n_i = 1.8 \times 10^5 \text{ cm}^{-3}$  (at 273 °K). Anodic current proceeds via dissolution of the gallium arsenide electrode:



This reaction is more negative than the oxidation of water,



and therefore occurs first. The anodic current is increased under illumination because of the generation of holes. The current is thus primarily dependent on the illumination level and independent of the applied voltage. This anodic dissolution of the electrode is not favorable in an ER experiment. In the case of gallium arsenide, the atomic arsenic which results from the dissolution, Eq. (1), forms a black coating on the surface. After about 15 min this coating is so thick that the electrode hardly reflects light. Thus, it is necessary to keep the operating voltages of the experiment such that cathodic current is drawn. Cathodic current occurs when the sample is biased negatively and the bands are pulled down to small depletion bending, flatband, or into accumulation. In this case the conventional explanation<sup>26</sup> for the current is that majority carriers (electrons) are forced towards the surface where they react with hydrogen ions, evolving hydrogen gas:



Illumination has no effect since it is a majority-carrier process. Work in progress by Benard<sup>27</sup>

indicates that a substantial portion of the cathodic current may be due to hole injection from the electrolyte. For ER purposes we need know only that flatband can be reached without severe dissolution of the electrode. It has been found that as long as the current drawn is net cathodic, the surface will remain clean, even though the dissolution process may occur during part of the modulation cycle.

For *p*-type GaAs in a sulfuric acid electrolyte the bands are also bent into depletion at the surface. For positive applied voltages (sample grounded, voltages measured relative to calomel in saturated KCl) anodic dissolution, Eq. (1), occurs very rapidly because of the large number of holes available as the bands are pulled up to flatband. Thus, flatband in *p*-type GaAs, reached at about 0.5-V positive bias, is accompanied by the arsenic-layer formation. This situation makes ER work on *p*-type GaAs unprofitable, at least in a sulfuric-acid electrolyte. The ER work reported here was done exclusively with *n*-type samples.

The cathodic currents drawn in large flatband modulations (square-wave voltages of several volts peak to peak), were often too large for the capabilities of the potentiostatic control system. Also, large cathodic currents are accompanied by much hydrogen evolution which interferes with the light beam being reflected off the interface. Regardless of what the current mechanism is, hole injection or electron extraction, it should be sensitive to the temperature of the electrolyte. Thus, in order to lower the currents drawn at the flatband position, the electrolyte was cooled down to  $(0 \pm 2)^\circ\text{C}$ . At this lower temperature, flatband could be reached while drawing less than 3 mA/cm<sup>2</sup> for all modulations used. At room temperature the cathodic current for a 1-V peak-to-peak flatband-to-depletion modulation was greater than 24 mA/cm<sup>2</sup>. The lower-temperature lower-current feature meant less gas evolution, and greater range of modulation voltages could be employed.

The sulfuric acid electrolyte was the only one tried in this work. Other work by D. Benard<sup>27</sup> had indicated that other acids or additions of other ions to the sulfuric acid to not provide better electrolytes for GaAs ER work. Furthermore, in a recently reported experiment<sup>14</sup> on GaAs using a non-aqueous electrolyte, saturated NH<sub>4</sub>NO<sub>3</sub> in ethyl alcohol, very poor ER results were obtained, galvanoluminescence being found to be quite important. Also in this work it was found that salt solutions lead to noticeable "dirtying" and destruction of the sample surface.

### C. Apparatus and Procedure

Single-crystal *n*-type gallium arsenide was obtained from the Monsanto Corporation. Doping levels in the range  $10^{14}$ – $10^{17} \text{ cm}^{-3}$  were used; how-

ever, most work was done on materials with doping levels of  $(1.2-2.4) \times 10^{16} \text{ cm}^{-3}$ .<sup>28</sup> The material was obtained as 0.030-in. slices cut to have a (111) face, a (110) face, or a (100) face. An Ohmic contact was made to the unpolished side using a gold lead and Au+12-at.-%-Ge discs<sup>29</sup> which form a eutectic with the gallium arsenide. The lead, back, and edge surfaces were coated with nonconducting epoxy. An etch composed of 50% concentrated sulfuric acid and 50% hydrogen peroxide was used. The electrolyte, 10%  $\text{H}_2\text{SO}_4$  in distilled water, was circulated in a closed loop through an ice-ethanol bath to produce a temperature of  $(0 \pm 2)^\circ\text{C}$  in the cell. The reference electrode for the potentiostatic control was calomel in 1 M KCl in water. The KCl solution made contact with the circulating electrolyte through a closed stopcock.

At the direct edge, Polaroid HR polyvinyl film was used as a polarizer. At higher energies, a Polaroid HNP'B film was employed. At the higher energies studied, 4–5.3 eV, narrow-bandpass filters made by Optics Technology were used to eliminate scattered light. Light emerging from the monochromator was directed onto the GaAs sample, separated from the quartz cell window by about 1 mm of electrolyte. Only enough deviation from normal incidence (less than  $15^\circ$ ) was used to enable separation of the beam reflected from the sample and the beam reflected from the quartz window. The reflected light was detected with an EMI 9684 S-1 response photomultiplier tube for energies below 2.0 eV and with an EMI 9558 S-20 response tube for energies above 2.0 eV.

The modulation and signal-processing electronics are shown schematically in Fig. 1. A potentiostat was used to maintain control over the dc bias of the sample and to ensure that the intended modulation waveform appeared at the sample. The modulation was a square wave of frequency  $\omega_1$  with a small sine wave of frequency  $\omega_2$  superposed on one-half of the square-wave cycle. Both signals were provided by the internal oscillators of Princeton Applied Research lock-in amplifiers. The square wave was typically 80 Hz and the sine wave 200 Hz. These signals were amplified, the sine wave gated, added, and fed into a Heathkit polarographic unit which served as the potentiostat. A Princeton Applied Research waveform eductor was also used to examine the  $\omega_2$  component of the photomultiplier signal. Sometimes the eductor was used to examine the  $\omega_1$  response in the ER signal for distortion from the desired square-wave form.

The ER response at the square-wave frequency was detected by the  $\omega_1$  lock-in and converted to logarithmic form using a Moseley logarithmic converter. The chart recording  $\Delta R/R$  data was digitized using an Autotrol 3400 curve tracer. A

Kramers-Kronig transformation of the  $\Delta R/R$  data was then performed by computer, and the values of the real and imaginary parts of the change in the dielectric constant,  $\Delta\epsilon_1$  and  $\Delta\epsilon_2$ , were determined from the results and the values of  $n$  and  $k$  for GaAs in the literature.<sup>30</sup>

### III. RESULTS AND DISCUSSION

ER measurements were made on several  $n$ -type samples over a 1.2–5.3-eV photon energy range. Some of the best results are shown in Fig. 2. We have identified six individual structures in the spectrum shown;  $E_0$ ,  $E_0 + \Delta_0$ ,  $E_1$ ,  $E_1 + \Delta_1$ ,  $E'_0$ , and  $E_2$ .<sup>1</sup> The data were obtained by three separate runs covering the three energy ranges 1.2–2.0, 2.0–3.8, and 3.8–5.3 eV. In the discussion below the direct-edge results will be presented first and used to discuss such points as the importance of flatband modulation and field inhomogeneity. The other structures will then be viewed in the light of the direct-edge results.

#### A. Direct-Edge Structures: $E_0, E_0 + \Delta_0$

The  $E_0, E_0 + \Delta_0$  line shapes shown in Fig. 2 arise from critical-point transitions from the three highest valence bands to the lowest conduction band at  $\Gamma$ . Because the energy band parameters at the direct edge are so well understood from other work,<sup>31,32</sup> the ER line shapes obtained here can serve as an excellent calibration of the entire experiment.

The importance of modulating from the flatband condition can be readily seen by examining the three

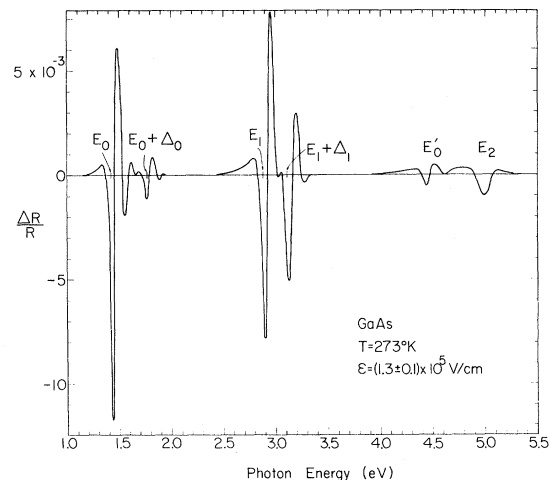


FIG. 2.  $\Delta R/R$  over the entire range of photon energies covered in this work. The sample used was  $n$ -type,  $1.2 \times 10^{16} \text{ cm}^{-3}$ . The electric field direction was [110] and the light unpolarized. The square-wave-modulation voltage  $V_{ac}$  was 4.0 V peak to peak. The corresponding  $\Delta\bar{\epsilon}$  obtained from a Kramers-Kronig transformation is shown in Figs. 8 and 9.

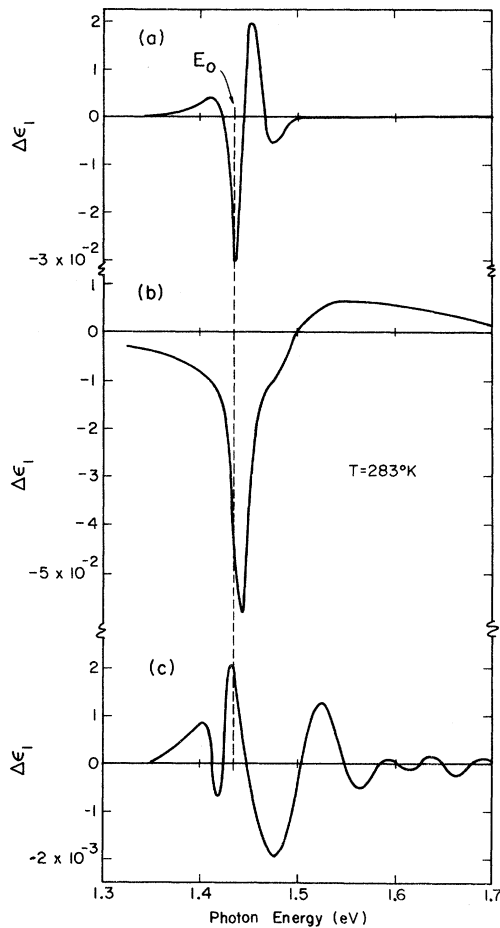


FIG. 3. The three curves presented here demonstrate the importance of dc bias on the ER spectra obtained at the direct edge  $E_0$ . All three curves were obtained with a 50-mV peak-to-peak square-wave modulation, however, with different dc bias voltages: curve (a) modulation from flatband to a depletion field; curve (b) modulation between two accumulation field values, the dc bias being approximately 100 mV toward accumulation from flatband; and curve (c) modulation between two depletion field values, the dc bias being approximately 3 V toward depletion from flatband. The sample was  $n$ -type,  $2.2 \times 10^{16} \text{ cm}^{-3}$ , field direction along [111] unpolarized light, temperature  $10^\circ \text{C}$ . Note that curve (c) has a smaller scale than curves (a) and (b).

$\Delta\epsilon_1$ ,  $E_0$  line shapes presented in Fig. 3. All three curves were obtained using a 50-mV peak-to-peak square-wave modulation; however, the dc voltage biases were quite different. Curve (a) in Fig. 3 results from a flatband-to-depletion modulation and clearly exhibits the shape of an electrooptic  $G_3$  function,<sup>22</sup> as it should for an  $M_0$  edge. Curve (b) was obtained with the dc voltage biased approximately 100 mV into accumulation from flatband. The shape of this curve is obviously much different from (a) and we believe arises from a non-Franz-Keldysh effect, such as band filling,<sup>17,33</sup> caused by

modulating into and out of degeneracy. Curve (c) results from modulation in the depletion side about  $3 V_{dc}$  from the flatband dc bias; note the scale difference between curves (c) and (a). This line shape is essentially a derivative with respect to field of a flatband-to-depletion line shape such as the one shown in Fig. 2. Line shapes such as (c) were the type obtained in our initial GaAs experiments. They are quite similar to the line shapes obtained in many of the earlier surface-barrier ER experiments on GaAs.<sup>3,4,8-11,14</sup> The three curves of Fig. 3 give a persuasive demonstration of the importance of knowing the relation of the applied voltage modulation to the flatband bias voltage. Without such knowledge, interpretation of the data is quite speculative. The presentation here of data obtained with accurate knowledge of the flatband position is the principal claim and result of this work.

Field inhomogeneity and thermal broadening effects, while certainly present and important to consider, were not found to be nearly as influential on our line shapes as had been found in much of the earlier ER work on GaAs.<sup>3,5,8-11,14</sup> This can be seen from the  $\Delta\epsilon_1$  line shape presented in Fig. 4. The plot shows  $\log_{10} \Delta\epsilon_1$  so that the oscillations can be seen over two decades. Each lobe in the line shape is a half-oscillation and is marked as positive or negative. Two perpendicular directions of the light polarization are shown. The value of the electric field given in Fig. 4, as well as all other field values quoted herein, was obtained by fitting a single electro-optic  $G_3$  function to the  $E_0 + \Delta_0$  structure<sup>34</sup> and assuming the effective masses for the conduction electron and  $\Gamma_7$  valence hole taken from the literature.<sup>31</sup>

The effects of field inhomogeneity on Franz-Keldysh line shapes have been demonstrated by Aspnes and Frova<sup>35</sup> for the special case of germanium and recently by Grover *et al.*<sup>23</sup> for a general case assuming a linear spatial field variation. The most obvious effects are a diminution of the size of subsidiary oscillations and a modification of the relative heights of the first few peaks in  $\Delta\epsilon$ . The effect depends upon the optical constants  $n$  and  $k$ , and is most pronounced for the case of  $k=0$ . Thus, we would expect field inhomogeneity effects to be most severe at direct-edge line shapes. For  $\Delta\epsilon_1$  at an  $M_0$  edge the most striking result of field inhomogeneity is the enhancement of the leading positive peak relative to the second positive peak. For a uniform field the ratio of the second positive peak to the leading positive peak in  $\Delta\epsilon_1$  should be about 8. However, with just a 40% drop in the field over the penetration depth of the light, the leading positive peak becomes equal to or slightly greater than the second positive peak.<sup>23</sup> The data of Fig. 4 show a ratio of about 7 for these peaks. The

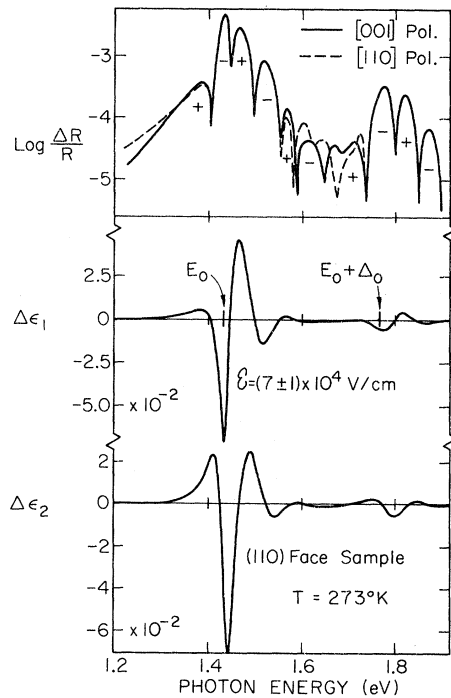


FIG. 4.  $\Delta R/R$  and  $\Delta\bar{\epsilon}$  for a [110]  $7 \times 10^{16}$ -V/cm field, two polarizations of the light.  $V_{ac} = 1.0$  V, peak to peak. The sample was  $n$  type,  $1.2 \times 10^{16}$   $\text{cm}^{-3}$ .

other direct-edge data presented here also show large ratios. This observation and the additional fact that many oscillations can be seen in the line shapes are good evidence that the fields achieved were quite uniform over the light penetration depth.

Koepfen and Handler<sup>36</sup> showed that field inhomogeneity could be minimized for a given field strength by modulating  $n$ -type samples into depletion and choosing the doping level so as to give the maximum length for the space-charge region. Their demonstration was for the equilibrium case in which minority carriers are permitted to build up as the surface field is increased until an inversion layer forms, severely limiting the length of the space-charge region. For the work reported here and the earlier work on Ge,<sup>15-17</sup> the equilibrium situation does not pertain. Instead, a substantial current is drawn which sweeps the minority carriers out of the space-charge region, preventing the formation of the inversion layer. Capacitance measurements on the  $n$ -type Ge :  $\text{K}_2\text{SO}_4$  system<sup>37</sup> and the  $n$ -type GaAs :  $\text{H}_2\text{SO}_4$  system confirm this hypothesis. Figure 5 shows capacitance curves, measured by D. Benard<sup>27</sup> in this laboratory, for  $n$ - and  $p$ -type GaAs in the  $10^{17}$ - $\text{cm}^{-3}$  doping range using 1- $M$   $\text{H}_2\text{SO}_4$ . Figure 5(a) shows the capacitance falling monotonically from cathodic biases above flatband (determined as  $-0.74$  V from the Shottky-Mott behavior of this curve) to

anodic biases of  $+2.0$  V. The dotted curve shows the expected behavior from the Poisson-Boltzmann law for the equilibrium case of inversion-layer formation. The germanium capacitance curves<sup>37</sup> show similar results. Figure 5(b) shows the situation for  $p$ -type GaAs in  $\text{H}_2\text{SO}_4$ . For  $p$  type we do get inversion since there is no process to sweep away the electrons, hence the turn-up of the capacitance curve. The sweeping away of the holes demonstrated by Fig. 5(a) is an important reason for the good near-uniform-field ER data reported in this work. The holes are all used in the anodic dissolution process, Eq. (1), resulting in a space-charge region that is quite deep even for the rather large surface fields reported here. Indeed, as can be seen in the capacitance curve of Fig. 5(a), the length of the space-charge region increases with field on the depletion side resulting in less field inhomogeneity for higher field values. Thus, in our experimental configuration, the effects of field inhomogeneity on the ER spectra can be minimized by modulating from flatband to a large depletion field. The dimensionless broadening can be seen to be small from the data of Fig. 4. The large number of oscillations observed and the narrowness of the first negative peak in  $\Delta\epsilon_1$  are indicative of a dimensionless broadening considerably smaller than one.<sup>2,12</sup>

An additional feature of interest in Fig. 4 is the polarization dependence of the line shape visible in the energy region 1.6–1.7 eV. This region is exhibiting an interference effect caused by the light- and heavy-hole contributions to the  $E_0$  structure. Since the transitions in this interference (beat) region take place away from  $\Gamma$ , the bands are no longer precisely isotropic, as they are right at  $\Gamma$ . This anisotropy leads to different dipole matrix elements for different light polarizations, since the dipole matrix elements are functions of the effective masses along the polarization direction.<sup>38</sup> Thus, the line shape in the beat region changes as the ratio of light-to-heavy hole matrix elements varies with light polarization. Unfortunately, the beat region in gallium arsenide occurs close to the spin-orbit split-off structure  $E_0 + \Delta_0$  at the field shown. Attempts to observe the beating at lower fields were not successful because the signal in the beat region was below the noise level.

There were two effects observed in the direct-edge experiments which are not understood. The first was an offset in the data for [100] and [111] field directions. This offset is indicated by arrows in Fig. 6 in the energy region above  $E_0 + \Delta_0$ , where the ER signal should vanish. The (100)-face data were taken with a  $1.2 \times 10^{16}$ - $\text{cm}^{-3}$  sample and the (111) with a  $2.3 \times 10^{16}$ - $\text{cm}^{-3}$  sample. The offset signal has the following properties: (i) magnitude comparable to the Franz-Keldysh oscillations in

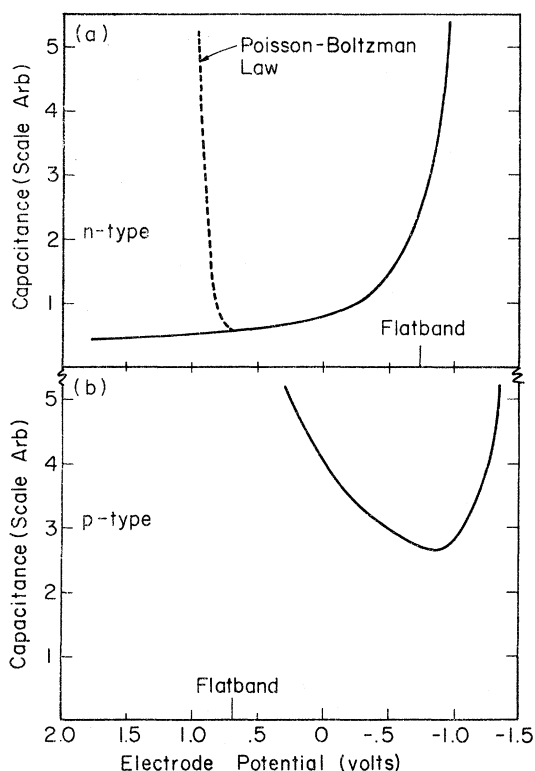


FIG. 5. Differential capacitance (scale arbitrary) for (a) *n*-type,  $3.7 \times 10^{17} \text{ cm}^{-3}$  and (b) *p*-type,  $2.0 \times 10^{17} \text{ cm}^{-3}$  in 1-*M*  $\text{H}_2\text{SO}_4$  at room temperature. The flatband voltages indicated were determined by extrapolation of the Shottky-Mott law behavior. The *p*-type curve (b) turns up for negative electrode potential indicating the formation of an inversion layer. The *n*-type capacitance curve (a) is monotonically decreasing however. If an inversion layer were to form in this case the capacitance would approximately follow the dashed curve. This monotonically decreasing capacitance, hence deepening space-charge region, means that relatively small field variation can be obtained over the light penetration depth encountered in the ER experiment.

the beat region; (ii) negative for [100] fields and positive for [111] fields; (iii) zero or below noise level for [110] fields; (iv) field dependence is slower than the Franz-Keldysh field dependence; (v) polarization independent; (vi) for [111] fields, very flat spectral dependence extending from the direct edge up to at least 4.2 eV; (vii) for [100] fields the spectral dependence is not as flat as the [111] fields, but dips below the noise level around 2.15 eV; (viii) magnitude changes with dc bias voltage somewhat (factor of 2). We do not understand the origin of this signal. Piezoelectrically induced piezoreflectance (PP) has been reported by Kyser and Rehn.<sup>13</sup> It is possible that the signal we observe arises in part from such an effect. The dependence upon the field direction, polarization dependence, and change with dc bias voltage support

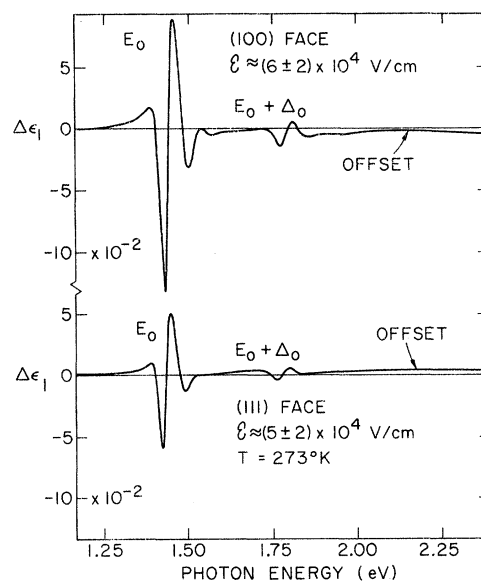


FIG. 6.  $\Delta\epsilon_1$  from data taken with a [100] field and a [111] field. The offset signal discussed in Sec. III A is indicated by arrows.

a PP hypothesis. However, the extremely broadband nature and large magnitude at  $E_0$ ,  $E_0 + \Delta_0$  argue against such an explanation.

Secondly, we point out in the  $\Delta\epsilon_1$  curve shown in Fig. 7 a depression in the positive leading edge around 1.36–1.40 eV. This is absent in the  $\Delta\epsilon_1$  curves for Figs. 3, 4, and 6, but may be seen in Fig. 2. We found that this flattening appears for

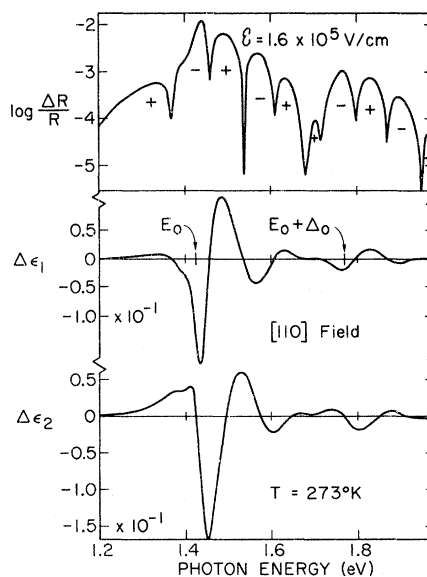


FIG. 7.  $\Delta R/R$  and  $\Delta\epsilon$  for a (110),  $1.6 \times 10^5 \text{ V/cm}$  field. The sample was *n* type,  $1.2 \times 10^{16} \text{ cm}^{-3}$ , the light unpolarized.  $V_{ac} = 5.0 \text{ V}$ , peak to peak.

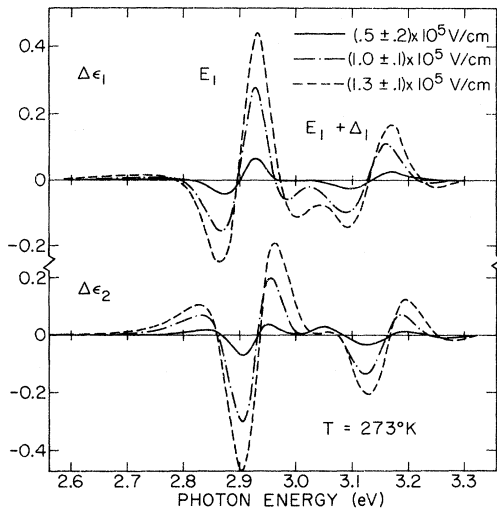


FIG. 8.  $\Delta\bar{\epsilon}$  from data taken with three different field magnitudes along a [110] direction. The sample was  $n$  type,  $1.2 \times 10^{16} \text{ cm}^{-3}$ , the light unpolarized.  $V_{ac} = (0.3, 2.0, 4.0) \text{ V}$ , peak to peak, respectively.

fields above  $9 \times 10^4 \text{ V/cm}$  and becomes more pronounced as the field is increased. We do not know what causes this effect. It may be related to the below-band-gap structures seen in the earlier work on GaAs.<sup>3, 4, 8-11, 14</sup>

The direct-edge data reported in Figs. 2-4, 6, and 7 were obtained under conditions of potentiostatic control and with good knowledge of the flat-band dc bias potential. The data exhibit the characteristics of nearly uniform field conditions. The effects of thermal broadening, while present, are not dominant. Hence, this data can be used with confidence in a quantitative analysis.

#### B. uv Structures: $E_1, E_1 + \Delta_1, E'_0, E_2$

$\Delta\bar{\epsilon}$  for the  $E_1, E_1 + \Delta_1$  structures is shown in Fig. 8 for three different values of the field strength. This pair of structures is known from piezoreflectance experiments<sup>39</sup> to arise from transitions along the [111] direction in the Brillouin zone. There has been considerable controversy over the type of critical point involved. A quantitative analysis of the data presented in Fig. 8 will be given in a later paper.<sup>18</sup> We note here, however, that the leading positive edge of  $\Delta\epsilon_2$  is quite large, as would be expected for an  $M_0$  type critical point. We know from the direct-edge data that the effects of field inhomogeneity are slight, even more so in this energy range than at the direct edge because of the shorter light penetration depth. Thus, the leading positive edge in  $\Delta\epsilon_2$  for the  $E_1$  structure could not be a nonuniform-field effect. The presence of this edge rules out  $M_1^{3D}$  type critical points. It will be shown in the analysis paper

that these structures are best represented by two-dimensional  $M_0$  edges implying that the region of  $k$  space responsible has cylindrical energy contours with the axis or infinite mass direction being along the [111] direction. This same conclusion was reached in earlier work on germanium.<sup>17</sup>

Figure 9 shows  $\Delta\bar{\epsilon}$  for the  $E'_0, E_2$  structures. The  $E'_0$  structure may actually be a pair of structures<sup>40</sup> but this cannot be determined from the data presented. The curves shown are for a [110] field direction and three different field strengths. It was found that there was some dependence on field direction. This can be seen from the curves of Fig. 10. These three different curves were obtained with different samples which may account for some of the differences in the ER signals. However, there must be some other effect, such as piezoelectrically induced piezoreflectance,<sup>13</sup> present besides the Franz-Keldysh effect to explain so large an orientation effect. In this photon energy range the thermal broadening should be so large as to wipe out differences in the Franz-Keldysh ER response caused by different field directions.

We found that in this photon energy range the conditions for flatband were rather different from those at  $E_0$  or  $E_1$ . Although the dc voltage bias was not too different ( $\sim 10\%$ ), the current was much lower than at either of the lower-energy structures, indicating that the electrical properties of our particular semiconductor-electrolyte system depend somewhat on the incident photon energy. Conditions which placed the sine-wave modulation

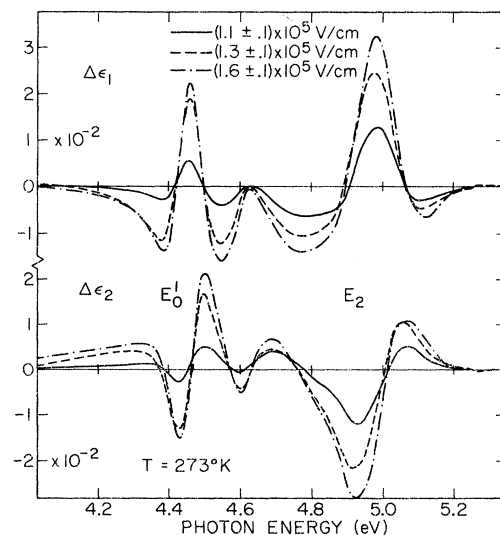


FIG. 9.  $\Delta\bar{\epsilon}$  in the 4.0-5.3-eV photon energy range. The field direction was [110], light unpolarized, sample,  $n$  type,  $1.2 \times 10^{16} \text{ cm}^{-3}$ .  $V_{ac} = (3.0, 4.0, 5.0) \text{ V}$ , peak to peak, respectively.



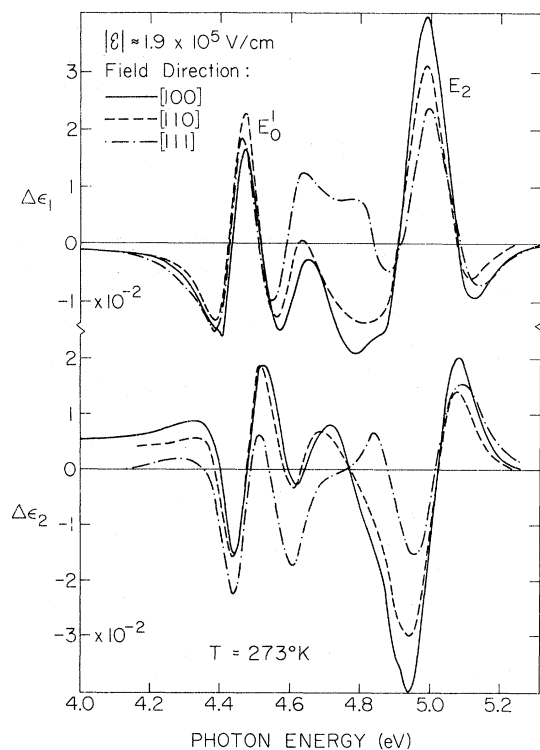


FIG. 10.  $\Delta\epsilon$  in the 4.0–5.3-eV photon energy range for three different field directions. The field magnitude of  $1.9 \times 10^5$  V/cm is approximate. The (100) and (110) data were taken with  $n$ -type  $1.2 \times 10^{16}$ -cm $^{-3}$  samples, the (111) data with an  $n$ -type  $2.3 \times 10^{16}$ -cm $^{-3}$  sample. The light was unpolarized.  $V_{ac} = 6.0$  V, peak to peak.

at the flatband position for the  $E_1$  photon energy range resulted in an accumulation position for our 4.0–5.3-eV runs. These off-flatband line shapes are quite different from those shown in Figs. 9 and 10. They exhibit fewer half-oscillations than the flatband curves. We could not duplicate the 6-V peak-to-peak modulation used for the curves in Fig. 10 at the  $E_0 + \Delta_0$  structure because of excessive currents. As a result we cannot calculate the field for the Fig. 10 line shapes by our usual method but estimate the field to be approximately  $1.9 \times 10^5$  V/cm by extrapolation of the calculations at smaller modulations.

#### IV. CONCLUSIONS

The purpose of this work was to obtain ER data for GaAs of sufficient quality to enable quantitative analysis. We have presented in the several figures above such data. The modulations are well characterized with respect to the flatband position. Potentiostatic control was employed. Square-wave modulations were used for all the data presented. Near-uniform fields were achieved by sweeping out the minority carriers from the space-charge region, frustrating the formation of an in-charge layer at high depletion fields. The effects of thermal broadening were present but not dominant at the direct edge. Broadening is, of course, much more important for the uv structures.

It will be shown in a later paper<sup>18</sup> that these data can be fit quite well with a one-electron theory.

\*Work supported, in part, by the Advanced Research Projects Agency under Contract No. HC 15-67-C-0221, the U. S. Army Research Office (Durham) under Contract No. DA-HC04-67-0025, and the Office of Naval Research.

† Present address: Xerox Research Laboratories, W-114, Rochester, N. Y. 14603.

<sup>1</sup>B. O. Seraphin and R. B. Hess, *Phys. Rev. Letters* **14**, 138 (1965).

<sup>2</sup>M. Cardona, *Solid State Phys. Suppl.* **11**, 1 (1969).

<sup>3</sup>B. O. Seraphin, *Proc. Phys. Soc. London* **87**, 239 (1966); *J. Appl. Phys.* **37**, 721 (1966).

<sup>4</sup>A. G. Thompson, M. Cardona, K. L. Shaklee, and J. L. Wooley, *Phys. Rev.* **146**, 601 (1966).

<sup>5</sup>F. H. Pollak, M. Cardona, K. L. Shaklee, *Phys. Rev. Letters* **16**, 942 (1966).

<sup>6</sup>V. Rehn and D. S. Kyser, *Phys. Rev. Letters* **18**, 848 (1967).

<sup>7</sup>J. D. Axe and R. Hammer, *Phys. Rev.* **162**, 700 (1967).

<sup>8</sup>E. W. Williams and V. Rehn, *Phys. Rev.* **172**, 798 (1968).

<sup>9</sup>F. H. Pollak and M. Cardona, *Phys. Rev.* **172**, 816 (1968).

<sup>10</sup>S. G. Dzhiioeva and V. B. Stopachinskii, *Fiz. Tekhn. Poluprov.* **3**, 386 (1969) [*Sov. Phys. Semicond.* **3**, 328 (1969)].

<sup>11</sup>T. Nishino, M. Okuyoma, and Y. Hamakawa, *J. Phys. Chem. Solids* **30**, 2671 (1969).

<sup>12</sup>R. A. Forman, D. E. Aspnes, and M. Cardona, *J. Phys. Chem. Solids* **31**, 227 (1970).

<sup>13</sup>D. S. Kyser and V. Rehn, *Solid State Commun.* **8**, 447 (1970).

<sup>14</sup>B. A. Bobilev, A. F. Kravhenko, Yu. V. Loburetz, and S. N. Salomon, *J. Appl. Phys.* **43**, 2320 (1972).

<sup>15</sup>P. Handler, S. Jasperson, and S. Koeppen, *Phys. Rev. Letters* **23**, 1387 (1969).

<sup>16</sup>S. Koeppen, P. Handler, and S. Jasperson, in *Proceedings of the Tenth International Conference on the Physics of Semiconductors, Cambridge, Mass., 1970* (U. S. AEC, Division of Technical Information, Springfield, Va., 1970), p. 422.

<sup>17</sup>S. Koeppen, P. Handler, and S. Jasperson, *Phys. Rev. Letters* **27**, 265 (1971).

<sup>18</sup>S. Pond and P. Handler (unpublished).

<sup>19</sup>K. L. Shaklee, F. H. Pollak, and M. Cardona, *Phys. Rev. Letters* **15**, 883 (1965).

<sup>20</sup>D. E. Aspnes and A. Frova, *Phys. Rev. B* **2**, 1037 (1970).

<sup>21</sup>Y. Hamakawa, P. Handler, and F. Germano, *Phys. Rev.* **167**, 709 (1968).

<sup>22</sup>D. E. Aspnes, *Phys. Rev.* **147**, 554 (1966); **153**, 972 (1967).

<sup>23</sup>J. Grover, S. Koeppen, and P. Handler, *Phys. Rev.*

B 4, 2830 (1971).

<sup>24</sup>D. B. Wittry and D. F. Kyser, *J. Phys. Soc. Japan Suppl.* 21, 312 (1966).

<sup>25</sup>V. Hein, in Ref. 16, p. 228; J. Scheer and J. Van Laar, *Surface Sci.* 18, 130 (1969).

<sup>26</sup>D. Elliot (private communication).

<sup>27</sup>D. Benard, Ph.D. thesis (University of Illinois, 1972) (unpublished).

<sup>28</sup>The doping levels stated here are the values quoted by the Monsanto Corporation at the time of purchase.

<sup>29</sup>Cominco Products, Inc., 818 W. Riverside Avenue, Spokane, Wash. 99201.

<sup>30</sup>R. C. Eden, Ph.D. thesis (Stanford University, 1967) (unpublished); available through University Microfilms Library Service Xerox Corp., Ann Arbor, Mich. 48106 as item No. 67-17415 R. C. Eden.

<sup>31</sup>Q. H. F. Vehren, *J. Phys. Chem. Solids* 29, 129 (1968); M. Reine, J. Aggarwal, and B. Lax, *Phys. Rev. B* 2, 458 (1970).

<sup>32</sup>M. D. Sturge, *Phys. Rev.* 127, 768 (1962).

<sup>33</sup>R. Glosser, J. E. Fischer, and B. O. Seraphin, *Phys. Rev. B* 1, 1607 (1970).

<sup>34</sup>The electric field could also be calculated from the modulation voltage values  $V_{ac}$  given in the figure captions since these are measured with respect to flatband. Thus, from straightforward application of Poisson's equation

we have for the surface field,  $\mathcal{E}_s = [(2en_D V_{ac})/\epsilon\epsilon_0]^{1/2}$ , where  $e$  is the electronic charge,  $n_D$  is the doping level, and  $\epsilon\epsilon_0$  is the permittivity. For example, the above equation gives a value of  $\mathcal{E}_s = 5.9 \times 10^4$  V/cm for the data shown in Fig. 4. Our fitting procedure gave  $\mathcal{E}_s = 7 \times 10^4$  V/cm. For the data of Fig. 7 the results are  $\mathcal{E}_s = 1.3 \times 10^5$  V/cm from the above equation and  $\mathcal{E}_s = 1.6 \times 10^5$  V/cm from our fitting procedure. A calculation using the modulation voltages measured with respect to flatband is equivalent to a calculation of the field using capacitance data. We believe that neither the above nor a capacitance calculation are as accurate as our values obtained from fitting the  $E_0 + \Delta_0$  structure.

<sup>35</sup>A. Frova and D. E. Aspnes, *Phys. Rev.* 182, 795 (1969); D. E. Aspnes and A. Frova, *Solid State Commun.* 7, 155 (1969).

<sup>36</sup>S. Koeppen and P. Handler, *Phys. Rev.* 18, 1182 (1969).

<sup>37</sup>S. Koeppen, Ph.D. thesis (University of Illinois, 1971) (unpublished).

<sup>38</sup>R. A. Smith, *Wave Mechanics of Crystalline Solids* (Wiley, New York, 1961) pp. 464-466.

<sup>39</sup>J. E. Wells and P. Handler, *Phys. Rev. B* 3, 1315 (1971).

<sup>40</sup>R. R. L. Zucca, J. P. Walter, Y. R. Shen, and M. L. Cohen, *Solid State Commun.* 8, 627 (1970).

## Electrical Properties of *n*-Type Epitaxial GaAs at High Temperatures

P. Blood

*Mullard Research Laboratories, Redhill, Surrey, England*

(Received 22 March 1972)

The Hall coefficient and Hall mobility have been measured in the temperature range 300–800 K on samples of *n*-type vapor-phase epitaxial GaAs from which the substrate has been removed by polishing to eliminate substrate conduction at high temperatures. The mobility varies as  $T^{-1.25}$  in the range 300–500 K and is compared with recent theoretical calculations. The thermal transfer of electrons from the  $\langle 000 \rangle$  to  $\langle 100 \rangle$  conduction-band minima is evident in the temperature dependence of both the mobility and the Hall coefficient, and the latter is used to derive the energy separation of these valleys as  $0.38 \pm 0.05$  eV using an analysis which minimises the effect of the temperature variation of the Hall scattering factor.

### I. INTRODUCTION

Conventional resistivity and Hall measurements have made an important contribution to the understanding of carrier transport processes in GaAs.<sup>1,2</sup> Earlier measurements were made on bulk-grown material, but more recently epitaxial layers of greater purity have been used for more detailed investigations.<sup>3,4</sup> For these electrical measurements the layers are grown on Cr-doped semi-insulating GaAs substrates which have a room-temperature resistivity of about  $10^8 \Omega \text{ cm}$ . In the usual specimen geometries of a long bar or clover leaf this substrate is electrically in parallel with the layer, but since the purest *n*-type layers have a room-

temperature resistivity of only  $10 \Omega \text{ cm}$  the conduction through the substrate is clearly negligible. In fact, this form of sample is quite satisfactory for measurements down to liquid-helium temperatures and a considerable amount of data in this range have been published.

In contrast to this situation, there is very little experimental data at elevated temperatures. Such measurements are limited to temperatures below  $600^\circ \text{C}$  by the evaporation of arsenic, although Roberts<sup>5</sup> has made measurements up to  $1190^\circ \text{C}$  on bulk crystals in an arsenic atmosphere. A more severe restriction to high-temperature measurements on epitaxial material is the rapid increase in conductivity of the substrate. Allen<sup>6</sup> has shown